An Experimental and Numerical Study of Polymer Action on Relative Permeability and Capillary Pressure

Patrick Barreau, Didier Lasseux, Henri Bertin, Philippe Glenat, Alain Zaitoun

Petroleum Geoscience, **5** (1999), 201-206, doi: 10.1144/petgeo.5.2.201

An experimental and numerical study of polymer action on relative permeability and capillary pressure

P. Barreau[1], D. Lasseux[1], H. Bertin[1], Ph. Glénat[2] and A. Zaitoun[3]

[1]*LEPT-ENSAM, University of Bordeaux I, Esplanade des Arts et Métiers, 33405 Talence Cedex, France*
[2]*TOTAL Exploration Production, Tour TOTAL, 24 cours Michelet, 92069 Paris La Défense Cedex, France*
[3]*Institut Français du Pétrole, 1–4 avenue de Bois Préau, 92852 Rueil Malmaison Cedex, France*

ABSTRACT: Unsteady state two-phase flow experiments were performed to check the action of an adsorbed water-soluble polymer on relative permeability and capillary pressure. A selective reduction of the relative permeability to water with respect to relative permeability to oil was observed. Capillary pressure, measured directly on the core, was increased after polymer injection. Since the polymer has little influence on interfacial tension, this trend is interpreted as a reduction of pore size due to polymer adsorption. The validity of this assumption was checked by the investigation of a pore-scale numerical model. Relative permeabilities and capillary pressure were computed for a range of flow rates. Numerical results indicated that the polymer adsorption model (wall effect) successfully reproduces qualitatively the experimental observations.

KEYWORDS: *porous media, polymer waterflooding, relative permeability, capillary pressure, boundary element (math)*

INTRODUCTION

Injection of polymer or gels in oil or gas production wells is commonly used, among other techniques, to reduce the water cut when excessive water production occurs. The success of this technique results from the blocking ability of hydrophilic polymers or gels to selectively reduce water relative permeability with respect to oil permeability. In spite of several experimental results on polymer or gel injection in various kind of porous media samples – sandstone, limestone, etc. – during the last decade (Schneider & Owens 1982; Zaitoun & Kohler 1987, 1988; Zaitoun *et al.* 1989; Dawe & Zhang 1994; Liang *et al.* 1994; Barreau *et al.* 1996; Liang & Seright 1997), the description of the physical mechanisms is still incomplete. In fact, if experimental results agree on the selective action of the polymer, several possible explanations of the phenomenon have been put forward (Liang and Seright, 1997): (i) shrinking of the gel, (ii) fluids partitioning, (iii) wall effect, (iv) wettability effect. In addition, most of the studies reported in the literature are focused on relative permeability and modification of end-point saturations and very little information is available on capillary pressure (Barrufet & Ali 1994). Even if capillary effects are generally of little interest near wells because of the dominance of viscous effects, this quantity can still provide useful information at the laboratory scale to help understand the physical mechanisms occurring during polymer injection and the resulting pore structure modification.

In this work, unsteady state oil–water flow experiments on water-wet sandstone cores were performed before and after the injection of polymer. Relative permeabilities were determined over the whole range of water saturation and capillary pressures were directly measured on the core.

Results of these experiments seem to indicate that a major effect of the polymer adsorption is a reduction in pore diameter. To check the phenomenological validity of this hypothesis, a pore-scale two-phase flow numerical model was run, allowing computation of relative permeabilities and capillary pressure.

EXPERIMENT

Materials and procedure

Polymer

A high molecular weight nonionic polyacrylamide (PAM) dissolved at 2500 ppm in a synthetic brine – 50 g l^{-1} KI, 0.4 g l^{-1} NaN_3 – was employed. After complete dissolution of the powder, the solution was filtered in order to remove any aggregates or microgel using a sequence of filters of 8 μm, 3 μm and 1.2 μm, respectively.

Oil

A mineral oil of 10.5 mPa s dynamic viscosity at room temperature was used. Interfacial tensions between oil and brine and between oil and polymer solution were respectively 33 N m^{-1} and 28 N m^{-1}.

Core sample

A Vosges sandstone of 0.25 μm^2 permeability and 23% porosity was used. A mineralogy study on this material showed a composition of quartz, feldspars and clays (7%), almost entirely covering the grains. Samples used in this study were 5 × 5 cm in section and 20 cm in length.

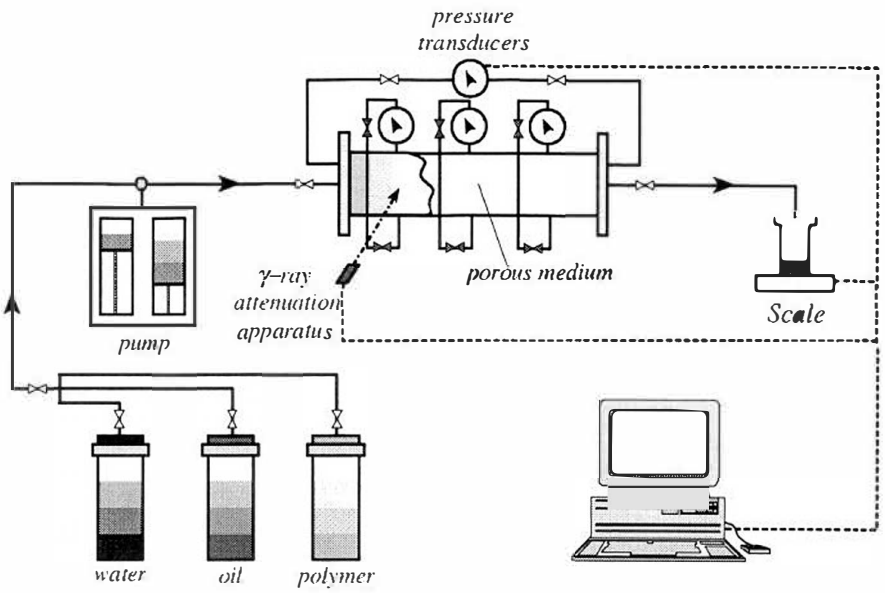

Fig. 1. Experimental setup.

Experimental setup

The experimental flow equipment, illustrated in Fig. 1, was placed in a temperature controlled area at 19 ± 1°C. Oil, brine and polymer solution, were injected in the porous medium by the means of an alternate syringe pump. The core was positioned horizontally on a two-dimensional rig moving a γ-ray attenuation device used to measure the *in situ* water saturation. Sixty equally spaced points placed along 4 rows and 15 columns were used as saturation measurement locations. Each saturation measurement corresponds to an averaged value across the sample thickness and the overall saturation map was obtained within 30 min. In addition to the *in situ* saturation measurements, pressure drop along the core and production at the outlet were measured continuously during the experiment. Moreover, capillary pressure was directly measured on the core during the inhibition processes using semi-permeable membranes. Three pairs of pressure taps were equally distributed along the sample. Each pair allowed a capillary pressure measurement in the same cross-section since pressures were respectively measured in the water phase through a hydrophilic membrane at the bottom and in the oil phase through a hydrophobic membrane at the top. Semi-permeable membranes were replaced after polymer injection to avoid plugging problems. Water saturations and pressure difference between wetting and non-wetting phases, i.e. capillary pressures, were always measured at the same intervals of time and same positions during the different cycles of each experiment.

Experimental procedure

Flow tests comprised seven main steps.

(1) The porous sample was carefully sealed at its periphery with an epoxy resin and glass fibre. Connectors for fluid injection were placed at each end and capillary pressure taps were positioned. The sample was vacuumed and then saturated with the brine. During this stage of the experiment, porosity and intrinsic permeability were measured.

(2) Oil flood at high flow rate ($Q_1 = 120$ cm^3 h^{-1}) was performed. At the end of this step, the irreducible water saturation, S^1_{wi}, and oil permeability, $K^1_o@S^1_{wi}$, were measured.

(3) Following the first drainage, a low flow rate ($Q_2 = 5$ cm^3 h^{-1}) water flood was performed. During this imbibition process, water saturation profiles, pressure drop, recovery and capillary pressure were measured during the overall displacement. At the end of this stage, the residual oil saturation, S^1_{or}, and the water permeability, $K^1_w@S^1_{or}$, were determined. At this point of the experiment, the sample was ready for a polymer treatment before a repeat of the same drainage/imbibition cycle.

(4) The polymer was injected in the sample at low flow rate, Q_2, and the adsorbed polymer fraction was estimated from the polymer front delay at the outlet relative to one pore volume injection time.

(5) The excess of polymer, non-adsorbed within the medium, was removed by injection of brine at Q_2. During this step, the residual oil saturation was unchanged, S^1_{or}, since no significant oil was produced and the water permeability, $K^2_w@S^1_{or}$, was determined. Semi-permeable membranes were replaced.

(6) A new drainage/imbibition cycle was started with an oil flood at high flow rate, Q_1. At the end of this second drainage, we measured the irreducible water saturation, S^2_{wi}, and oil permeability, $K^2_o@S^2_{wi}$.

(7) Finally, a second imbibition was performed at flow rate Q_2 characterized by a residual oil saturation, S^2_{or}, and water permeability $K^2_w@S^2_{or}$.

Experimental results

Our results are presented in terms of (a) adsorbed polymer layer thickness, and (b) oil/water front displacement, water saturations, relative permeabilities and capillary pressure comparisons before and after polymer treatment.

The adsorbed polymer quantity was estimated to be 97 μg g^{-1} leading to a polymer layer thickness of 0.49 μm (Barreau *et al.* 1996). This is in agreement with previous work (Zaitoun & Kohler 1989).

End-point data before and after polymer injection are summarized in Table 1 and indicate that irreducible water saturation is significantly higher after polymer adsorption, while residual oil saturation is almost unchanged. The higher water saturation after polymer injection can be explained by polymer water

Table 1. *End-point data before and after polymer*

S^1_{wi}	$K^1_o@S^1_{wi}$ (μm^2)	S^1_{or}	$K^1_w@S^1_{or}$ (μm^2)	$K^2_w@S^2_{or}$ (μm^2)	S^2_{wi}	$K^2_o@S^2_{wi}$ (μm^2)	S^2_{or}	$K^2_w@S^2_{or}$ (μm^2)
0.327	0.222	0.336	0.0155	0.00142	0.492	0.138	0.328	0.0007

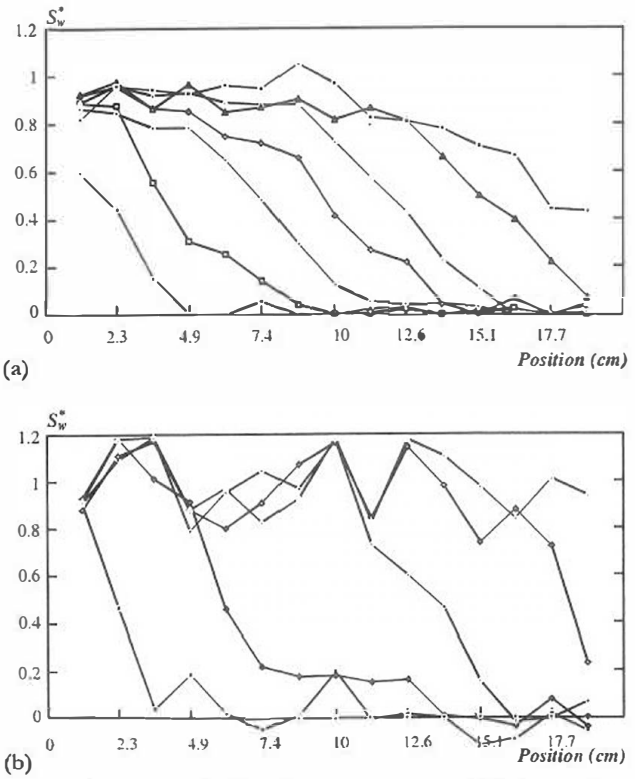

Fig. 2. Experimental reduced water saturations (a) before polymer injection, (b) after polymer injection.

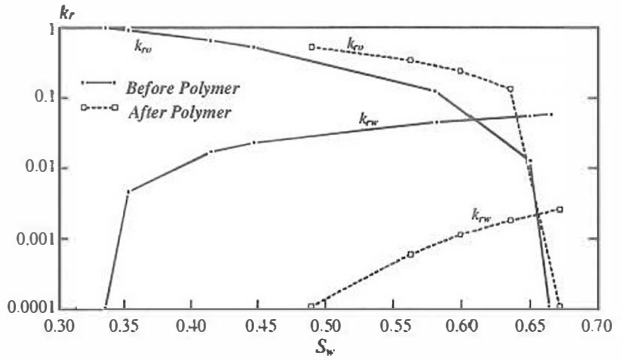

Fig. 3. Capillary pressure as a function of water saturation before and after polymer adsorption.

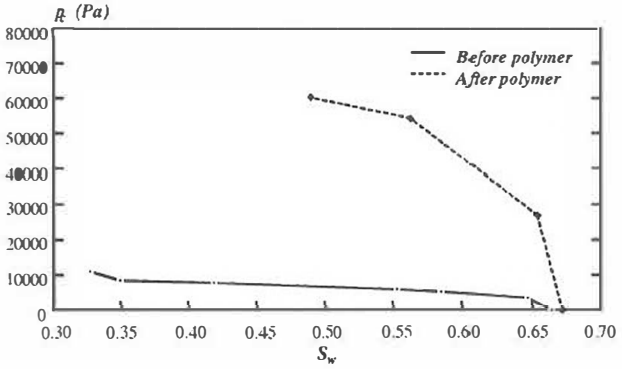

Fig. 4. Modification of water and oil relative permeabilities before and after polymer injection.

hydration but also by the fact that smaller pores, which are water-saturated, have been closed to oil.

Figures 2a and b illustrate the reduced water saturation profiles – averaged over four points in the same cross-section – before and after polymer adsorption. The reduced saturation is given by the relationship:

$$S^{*j}_w = \frac{(S^j_w - S^j_{wi})}{(1 - S^j_{or} - S^j_{wi})} \quad \begin{matrix} (j=1\text{: before polymer;} \\ j=2\text{: after polymer)} \end{matrix} \qquad (1)$$

We note that the displacement front is spread out much more in the absence of adsorbed polymer than in the presence of it. This can be understood as a result of the balance between viscous and capillary effects. Capillary pressure relationships measured before and after polymer adsorption are plotted in Fig. 3. In addition to the above-mentioned increase in the initial water saturation, a dramatic increase in capillary pressure after polymer adsorption over the whole saturation range can be observed. Since interfacial tension between oil and water on the one hand and oil and polymer solution on the other hand are almost the same, the increase in capillary pressure is representative of pore throat size reduction when polymer is adsorbed. This is easier to conceptualize if a simple bundle of capillary tubes is used to represent the porous medium. The capillary pressure, which is proportional to the interfacial tension and wetting angle and inversely proportional to the tube radius, can only be increased if the tube diameter is reduced, keeping all other parameters constant. This effect will be examined in more detail in the subsequent numerical study.

The relative permeabilities in Fig. 4, normalized by $K^1_o@S^1_{wi}$, were determined using a minimization software – FISOLE℠ – (Chardaire *et al.* 1989) that simultaneously estimates relative permeabilities and capillary pressure from experimental measurements. In this case, we used recovery, pressure drop, saturation profiles and capillary pressure as experimental data to determine the relative permeabilities. From these estimations, the ratio between oil relative permeabilities – at irreducible saturation S^2_{wi} – before and after polymer adsorption is equal to 0.8, while the ratio between water relative permeabilities – at the residual saturation, S^1_{or} – is equal to 22.5. Several drainage-imbibition cycles in the absence of polymer were performed on a similar core and a very weak hysteresis effect was found (Barreau 1996). This excludes an experimental artefact of this kind and confirms the selective action of the polymer.

NUMERICAL TESTS

The above results on both capillary pressure and relative permeabilities suggest, in addition to other effects mentioned in the literature (Zaitoun & Kohler 1988; Liang & Seright 1997),

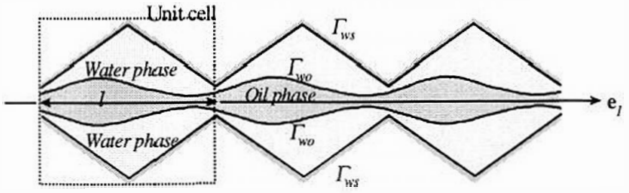

Fig. 5. Pore model geometry.

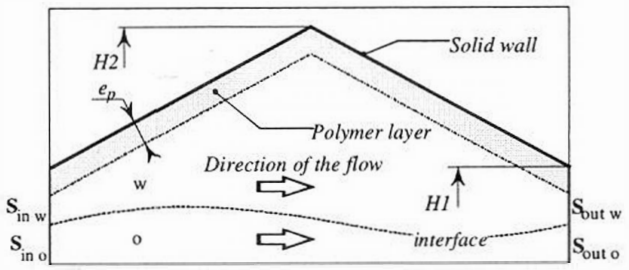

Fig. 6. Domain configuration for computation.

that a possible mechanism to explain such behaviour is a reduction of the pore diameter due to polymer adsorption. The validity of such a hypothesis was checked by performing numerical two-phase flow experiments on a model 2D pore geometry. Rather than reproducing direct experimental configurations, the goal of this part of the work was to investigate the phenomenology of the process.

Geometry and hypotheses

The model pore geometry used in this study consists of a water-wet infinite succession of two-dimensional, periodic, of period $l\mathbf{e}_1$, convergent–divergent cells in which the oil-phase (o) flows trough the centre (Fig. 5). Gravity is assumed to have a negligible contribution compared to viscous and capillary effects and we solved the two-phase Stokes flow resulting form the application of an external pressure gradient, $h\mathbf{e}_1$, in the axial direction in the computational domain shown in Fig. 6. The solution of this problem depends on the five following parameters: the water saturation, S_w; the water to oil viscosity ratio, μ_w/μ_o; the ratio of capillary to external applied forces; $\gamma/h l^2$ where γ is the oil/water interfacial tension; and geometrical dimensionless characteristics, *H1* and *H2*, of the cell (see Fig. 6). To simulate the presence of the polymer, it was assumed, for simplicity, that the adsorbed polymer layer is immobile and fully water saturated with a constant thickness, e_p, as depicted in Fig. 6.

Method and algorithm

The two-phase flow is solved using a boundary element technique after the boundary value problem has been reformulated in its equivalent integral form (Ladyzhenskaya 1969; Pozrikidis 1992; Barreau *et al.* 1994; Barreau 1996). First, the oil–water interface, satisfying mass and momentum balance equations according to the applied pressure gradient, was sought iteratively (Barreau 1996). Once this stationary solution has been reached, relative permeabilities, $k_{r\alpha}$, and capillary pressure, P_c, were computed according to the dimensionless formulae (Barreau *et al.* 1997):

$$k_{r\alpha} = -\left(l^3 \sum_{S_{in\,\alpha}} \mathbf{v}_\alpha \cdot \mathbf{e}_1 \Delta l \right) \Big/ k_e A_\alpha \quad \alpha = \mathrm{w,o} \qquad (2)$$

$$P_c = \gamma/h l^2 \langle C \rangle |\Gamma_{wo} \qquad (3)$$

where $S_{in\alpha}$ is the portion of the cell entrance within the α-phase, v_α the α-phase dimensionless velocity, Δl the boundary element length, k_e the effective permeability to oil in the absence of polymer at the irreducible water saturation, A_α the area of the computational domain occupied by the α-phase and $\langle C \rangle |\Gamma_{wo}$ the double mean curvature along the stationary interface Γ_{wo}.

Identical calculations were performed without any adsorbed polymer layer in a first step and in the presence of the polymer layer in a second step, leading to a reduction of *H1* and *H2*, i.e. of the pore diameter, in accordance with e_p. The overall procedure was repeated for increasing water saturations, reproducing a complete steady-state imbibition process.

Results

Computational results presented below were obtained with the following quantities made dimensionless by the period l (see Fig. 5): $H1=0.417$, $H2=0.167$, $e_p=0.05$ and $\mu_w/\mu_o = 9.09 \times 10^{-2}$ which corresponds to an oil with a dynamic viscosity of 11 mPa s.

Irreducible water saturation

The irreducible water saturation is systematically higher after polymer is introduced in the model. Although this directly follows from our hypothesis of a fully water saturated polymer layer, this is in accordance with experimental observations.

Relative permeabilities

Relative permeability results obtained for $\gamma/h l^2 = 0.1$, 1 and 10 are represented in Fig. 7 as functions of the water saturation. These data clearly indicate that the simplified model used here for the adsorbed polymer layer is able to reproduce a selective action since the relative permeability reduction is roughly twice as large for the water-phase than for the oil-phase at $S_w = 0.7$ (see Table 2). This selective behaviour increases with $\gamma/h l^2$.

Capillary pressure

Capillary pressure curves obtained with $\gamma/h l^2 = 1$ and computed from Eqn 2 are represented in Fig. 8 as functions of the water saturation. The capillary pressure modification induced by the reduction of the pore diameter is in accordance with our experimental observation. In fact, after the polymer layer has been introduced, the capillary pressure is strongly increased indicating that the pore diameter reduction yields a significant increase in the mean curvature of the oil–water interface.

CONCLUSIONS

The effect of adsorbed polymer on oil–water flow was studied from direct experiments on sandstone cores. As previously reported in the literature, our experiments indicate that:

(1) irreducible water saturation increases after polymer has been injected. This can be explained by a (small) contribution of polymer hydration water and mainly by the fact that smaller pores are closed to oil flow;

(2) relative permeability curves clearly exhibit the selective action of the polymer since the relative permeability of the water is much more reduced than the relative permeability of the oil.

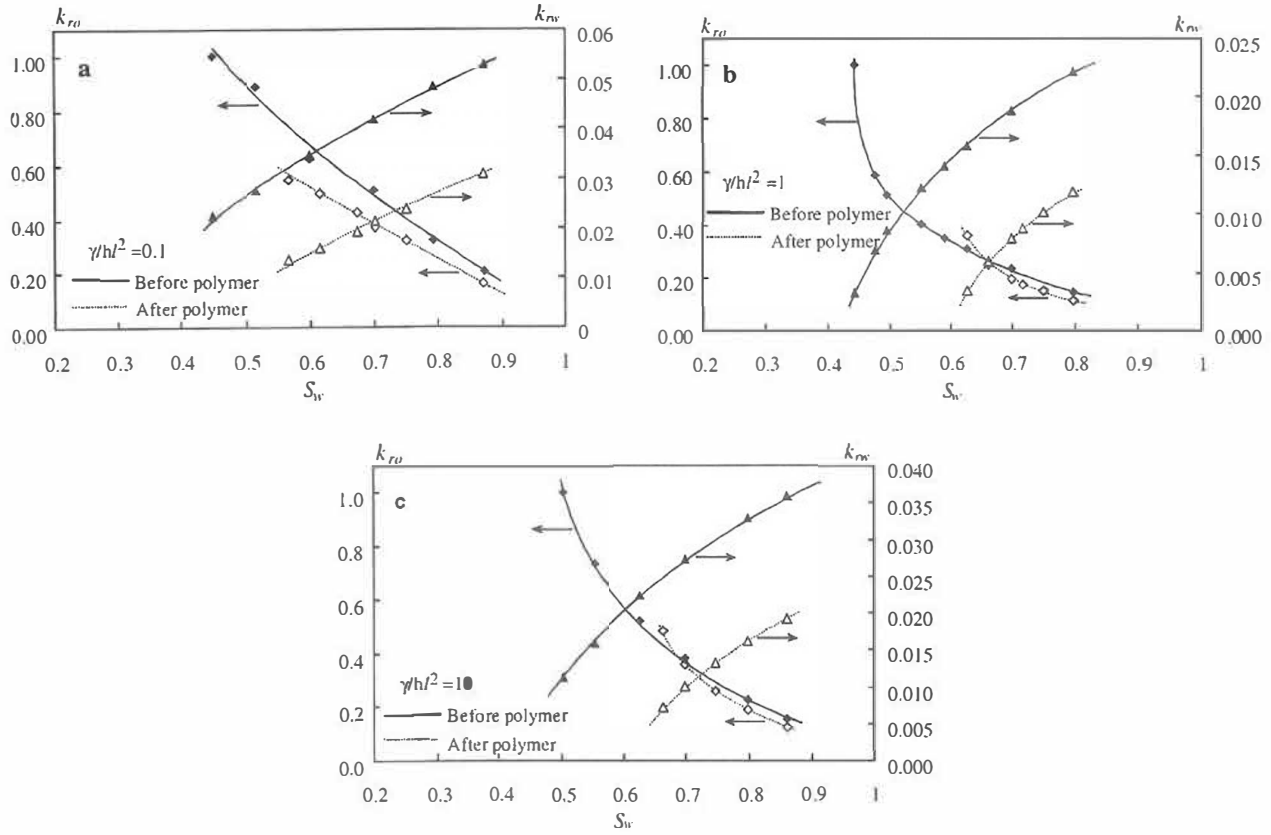

Fig. 7. Computed relative permeabilities before and after polymer injection.

Table 2. *Computed relative permeabilities, before and after polymer, at S_w=0.7 on a model-pore geometry*

	$\gamma/h/^2=0.1$		$\gamma/h/^2=1$		$\gamma/h/^2=10$	
	k_{rw}	k_{ro}	k_{rw}	k_{ro}	k_{rw}	k_{ro}
Before polymer	0.0417	0.5074	0.0188	0.235	0.0273	0.3834
After polymer	0.0215	0.3710	0.0079	0.196	0.0101	0.3594
k_r reduction	1.94	1.37	2.38	1.20	2.70	1.07

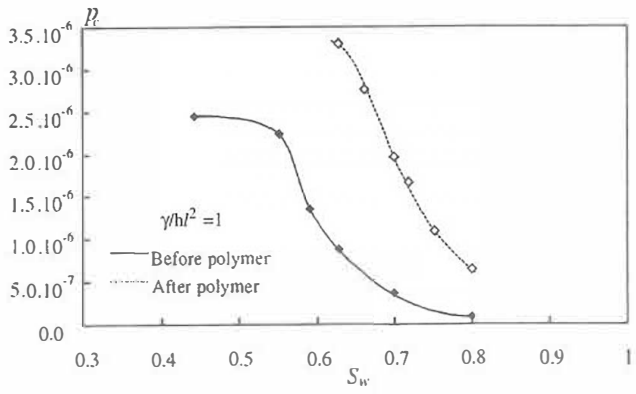

Fig. 8. Computed capillary pressure before and after introduction of the polymer layer.

(3) our direct measurements showed that the presence of adsorbed polymer yields a strong capillary pressure increase.

(4) a comparison of *in situ* water saturation evolutions, indicates that the oil/water front is spread out much more without polymer than in the presence of it. At a first glance, one could believe that this is indicative of a capillary pressure decrease after polymer adsorption. However, one must be very careful when drawing this kind of conclusion since the shape of the oil/front is intimately related to the product of relative permeability and capillary pressure derivative with respect to the saturation. In this case, both relative permeabilities and capillary pressure are modified by the adsorbed polymer and the experimental evidence is that the capillary pressure is actually increased by the presence of the polymer. This behaviour is confirmed by direct numerical simulations performed with FISOLE®, using our experimental data.

All these results suggest that a significant mechanism is a net pore size reduction resulting from the adsorbed polymer layer (wall effect). The phenomenological validity of this hypothesis was checked with the aid of a numerical model. Making using of a simplified polymer layer model, direct pore-scale numerical simulations of oil–water flow were performed in a model-pore geometry. They correctly reproduce phenomena observed experimentally.

Financial support provided by Groupement Scientifique ARTEP (ELF EP, Institut Français du Pétrole, TOTAL and Gaz de France) and CNRS is gratefully acknowledged.

REFERENCES

BARREAU, P. 1996. *Modifications des propriétés polyphasiques d'un milieu poreux en présence d'une couche de polymère adsorbé: études expérimentale et numérique*. PhD thesis, ENSAM Bordeaux.

——, BERTIN, H., LASSEUX, D., GLÉNAT, Ph. & ZAITOUN, A. 1996. Water control in producing wells: Influence of an adsorbed polymer layer on relative permeabilities and capillary pressure. Paper SPE 35447, presented at the Symposium on Improved Oil Recovery, Tulsa, Oklahoma.

——, LASSEUX, D., BERTIN, H., GLÉNAT, Ph. & ZAITOUN, A. 1997. Polymer adsorption effect on relative permeability and capillary pressure: investigation of a pore scale scenario. Paper SPE 37303, presented at the International Symposium on Oilfield Chemistry, Houston.

——, ——, —— & ZAITOUN, A. 1994. Effect of adsorbed polymer on relative permeability and capillary pressure: a pore scale numerical study. *In*: Brebbia, Kim, Oswald and Power, (eds) *BEM XVII*. Comp. Mech. Pub., Southampton, 549–556.

BARRUFET, M. A. & ALI, L. 1994. Modification of relative permeability curves by polymer adsorption; Paper SPE 27015, presented at Buenos Aires, Argentina.

CHARDAIRE, C., CHAVENT, G., JAFFRÉ, J., LIU, J. & BOURBIAUX, B. 1989. Simultaneous estimation of relative permeabilities and capillary presure. Paper SPE 19680, presented at the 64th Annual Technical Conference and Exhibition, San Antonio, Texas.

DAWE, R. A. & ZHANG, Y. 1994. Mechanistic study of the selective action of oil and water penetrating into a gel emplaced in a porous medium. *Journal of Petroleum Science and Engineering*, **12**, 113–125.

LADYZHENSKAYA, O. A. 1969. *The mathematical theory of viscous incompressible flow*. Gordon & Breach, New York.

LIANG, J. & SERIGHT, R. 1997. Further investigations of why gels reduce K_{rw} more than K_{ro}. Paper SPE 37249, presented at the International Symposium on Oilfield Chemistry, Houston, Texas.

——SUN, H. & SERIGHT, R. S. 1994. Why do gels reduce water permeability more than oil permeability. Paper SPE/DOE 27829, presented at the Symposium on Improved Oil Recovery, Tulsa, Okalahoma.

POZRIKIDIS, C. 1992. *Boundary integral and singularity methods for linearized viscous flow*. Cambridge University Press.

SCHNEIDER, N. & OWENS, W. W. 1982. Steady-state measurements of relative permeability for polymer/oil systems. *Society of Petroleum Engineers Journal*, **9408**, 79–86.

ZAITOUN, A. & KOHLER, N. 1987. The role of adsorption in polymer propagation through reservoir rocks. Paper SPE 16274, presented at the International Symposium on Oilfield Chemistry, San Antonio, Texas.

—— & —— 1988. Two-phase flow through porous media: effect of an adsorbed polymer layer. Paper SPE 18085, presented at the 63rd Annual Technical Conference and Exhibition, Houston, Texas.

—— & —— 1989. Modification of water/oil and water/gas relative permeabilities after treatment of oil or gas wells. *In Situ*, **13**, 55–77.

——, —— & GUERRINI, Y. 1989. Improved polyacrylamide treatments for water control in producing wells. Paper SPE 18501, presented at the International Symposium on Oilfield Chemistry, Houston, Texas.